Palladium Nanotubes for Optical Hydrogen Sensing

The Fabrication and Characterisation of Arrays of Nanostructures

M. B. McAuley, A. Murphy, R. Pollard
Centre for Nanostructured Media, IRCEP
The Queen's University of Belfast
Belfast, BT7 1NN, United Kingdom
mmcauley14@qub.ac.uk

Abstract— **Arrays of freestanding upright palladium nanotubes have been fabricated using a bottom-up method of electrodepositing into anodised alumina pores. Optical transmission measurements carried out with a range of post-fabrication treatment methods suggest that hydrogen diffuses into both the inner and outer surface areas of the tube structure. Furthermore, scanning electron microscopy of the same sample before and after cycling hydrogen exposure show that the structures appear undamaged by the repeated lattice expansion.**

Keywords-component; optical sensing; gas sensing; palladium; hydrogen; nanotubes

I. INTRODUCTION

The present interest in hydrogen sensing materials has been driven by the increasing requirement for detection in emerging fuel and energy storage technologies. With an explosive limit of 4% in air, there is a necessity to produce faster and more sensitive sensors. Hydrogen sensors in their simplest form detect optical [1-2] or resistance [3] changes in a palladium thin film upon absorption and diffusion of H atoms: optical methods are favoured for safety applications due to the risk of ignition from electrical connections [4].

At a sufficiently close distance to palladium, a hydrogen molecule undergoes physisorption to the surface. If it has adequate energy, the molecule will become dissociated and chemically bind to the surface, from where it can then diffuse further into the face centre cubic (fcc) palladium lattice[5].

The thin film sensing element construction has a number of drawbacks [6]. Firstly, a compromise exists between sensitivity and reaction time dependent upon the thickness of the film. Diffusion through thicker films is slower, but offers a greater signal change, whereas the hydrogen atoms diffuse quickly though a thin film offering a more rapid signal change of smaller magnitude. Secondly, long-term stability is reduced by degradation of the film through expansion and contraction upon repeated hydrogen diffusion, manifesting in blistering and buckling [7-8]. In order to overcome these difficulties and to improve overall sensor performance, the current interest focuses on nanostructured materials to achieve simultaneous speed and sensitivity through both individual structures [9-10] as well as larger, scalable arrays of structures [11-12].

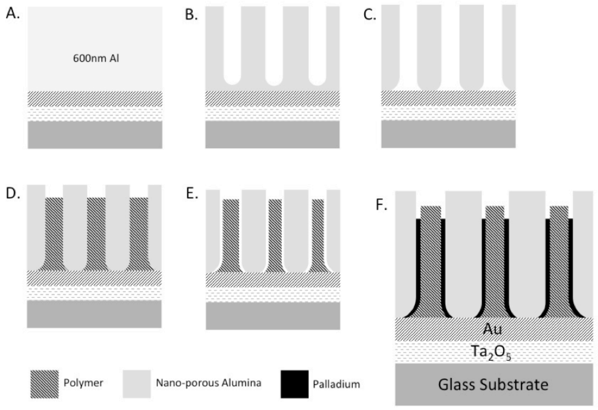

Figure 1. Cross-sectional schematic of the nanotube fabrication process. The completed nanostructures are shown (F) in their template, with the intermediate stages of the process given by (A)-(E). The process begins with sputtering a multi-layer film consisting of Ta_2O_5, Au and Al on a glass substrate (A), followed by anodisation to produce an array of nanopores (B). A NaOH chemical etch removes the alumina remaining at the base of the pore (C), allowing a polymer to be electro-deposited (D). A further chemical etch widens the pore around the polymer (E), into which the palladium can be electro-deposited (F).

II. FABRICATION

A. Fabricating arrays of nanotubes

A schematic of the nanotube fabrication process is presented in Fig. 1. A glass substrate was prepared via magnetron sputtering of a Ta_2O_5 adhesion layer and a gold electrodeposition seed layer, followed by a layer of aluminium (A). Anodising, this formed an array of uniform pores in alumina (B) and a NaOH chemical etch used to remove the remaining alumina at the base of the pores and reveal the gold layer (C). This acts as a seed layer, onto which a sacrificial polymer nanorods were electrodeposited from monomer in an electrolyte (D) [13]. The pores were widened with a further chemical etch (E), leaving a template into which palladium was electrodeposited to form the nanotube structures (F). The samples used in this investigation had an average outer diameter of 60nm and height of 200nm. The nature of the fabrication process allowed good control over the aspect ratio,

---

Funded by Department for Employment and Learning Northern Ireland

wall thickness and spacing of the structures through electrodeposition time, duration of chemical etching and anodisation voltage respectively.

B. Post fabrication techniques

Post-fabrication treatments allow removal of both the alumina template and the polymer core through chemical and plasma etches respectively. This produces a selection of samples (Fig. 2) that selectively expose the inner and outer surfaces of the nanotube.

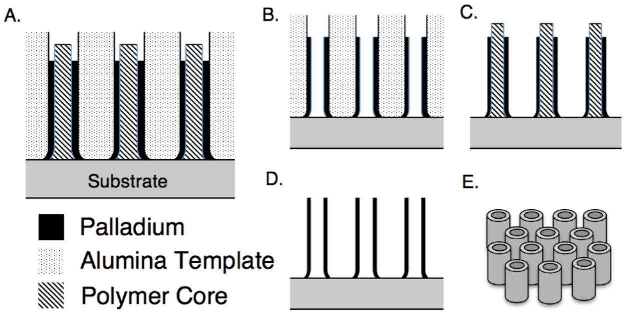

Figure 2. Cross-sectional schematic of a range of samples that have been treated post-fabrication to selectively expose the inner and outer surfaces of the nanotube: No Treatment (A), Core removed (B), Template removed (C), Template and Core removed (D) and 3D view with the Template and Core removed (E).

III. CHARACTERISATION SYSTEM

The home-built test system (Fig. 3) offers fully automated exposure to various cycle profiles of hydrogen with simultaneous acquisition of transmission data through the test sample. Two Mass-Flo Controllers (MFC1 and MFC2) flowing nitrogen and hydrogen are used to allow a wide range of hydrogen concentrations, monitored within the control program. Pressure and flow meters (PRC1 and MFM1) maintain a pressure at the inlet of a third controller, MFC3, providing a steady flow rate through to the specially designed exposure chamber with the sample held inside. Glass viewing ports allow for optics to be mounted outside the chamber; a 617nm LED is incident on the sample inside and a signal proportional to transmission is acquired via a photodiodes. At the inlet of MFC1, a three-way valve allows selection between pure nitrogen and a pre-mixture of 2% hydrogen in nitrogen. Another procedure of the control program compares the sample response between the system mix and pre-mix gas to verify functionality.

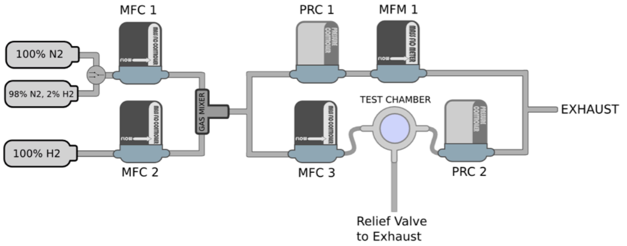

Figure 3. Schematic of the characterisation system showing Mass-Flo Controllers (MFC), Pressure Controllers (PRC) and a Mass-Flo Meter (MFM) arranged to produce a steady gas flow and pressure of a controlled concentration of hydrogen in nitrogen, though a test chamber.

IV. RESULTS

To better understand the absorption kinetics of the nanotubes, a range of identical structures with different post-fabrication treatments were exposed to a fixed amount of hydrogen and the change in transmission compared, with sensitivity defined as

$$Sensitivity\ (\%) = \frac{T_H - T_N}{T_N} \times 100 \qquad (1)$$

where T_N and T_H are the transmission photodiode voltages during nitrogen and hydrogen exposure.

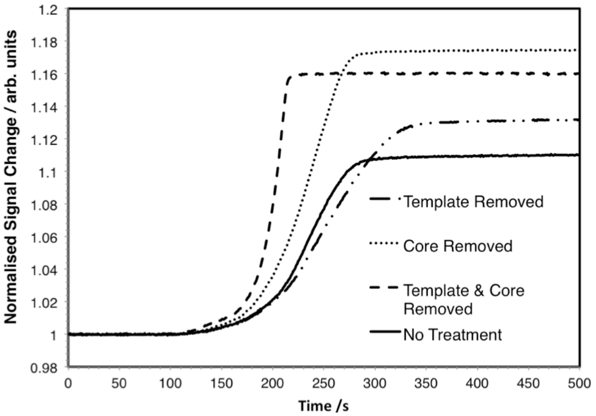

Figure 4. Normalised sensor response for a range of identical Palladium nanotube arrays with different post-fabrication treatments.

Combinations of chemical and plasma etch treatments produced samples of nanotubes with the core and template removed, only the core removed and only the template removed. The sensitivity in transmission of each, as defined in Eq. 1, is shown in Fig. 4, normalised to hydrogen

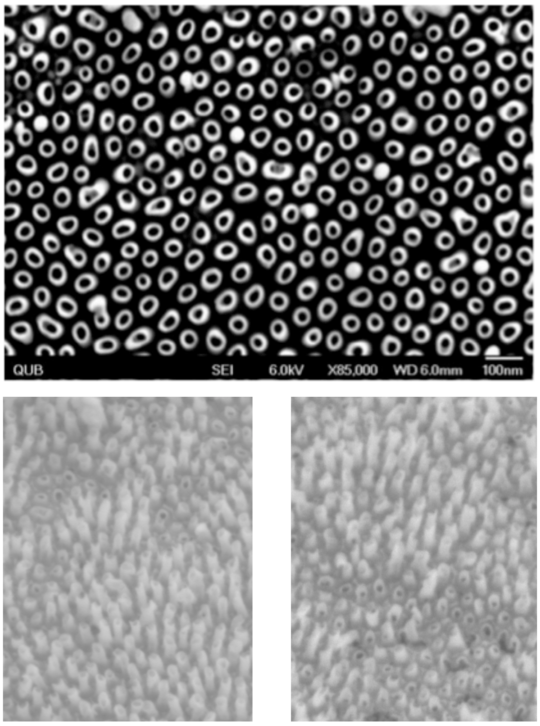

Figure 5. SEM images of palladium nanotubes (top) and similar areas on a single Palladium nanotube sample before (bottom left) and after (bottom right) 80 cycles of 1-2% hydrogen in nitrogen. Regions that are not fully formed are present before cycling and are artifacts of the fabrication process.

exposure at 100s, along with an untreated sample for comparison. There are two features of this figure that should be compared between samples; the maximum amplitude, indicative of sensitivity and the gradient of the slope, indicative of the reaction time to achieve this signal change. By removing only the template, the maximum amplitude increases with little change in the gradient; whereas removing only the core, the maximum amplitude and gradient increase significantly. The greatest improvement on the untreated samples is apparent when both the template and core are removed, suggesting that new adsorption sites are opened up by this treatment as well as absorption into a greater amount of palladium.

The structures offer an additional advantage over thin films in their ability to expand and contract into the gaps between the nanotubes, leading to a reduction in blistering. By examining SEM images of similar areas on a single sample before and after 80 cycles of 1-2% hydrogen, we observed no significant change in the structures. Regions of the sample that are not fully formed are present before cycling with hydrogen and are artifacts of the fabrication process.

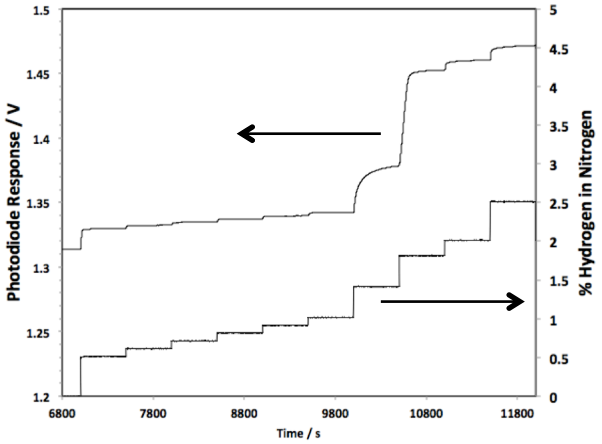

Figure 6. Photodiode response of nanotubes transmission (primary axis) for a stepped exposure profile (secondary axis).

Having discussed the absorption kinetics and advantages of using nanostructures, we now present a further characterisation of the structures. By exposing the structures to a stepped exposure profile as in Fig. 6, we can easily extract the sensitivity response from a range of hydrogen concentrations by using the baseline voltage at the beginning of the sequence as T_N and the maximum voltage at each step as T_H. Plotting this sensitivity against the hydrogen concentration in Fig. 7, the locations of the alpha and beta phase regimes become apparent. The region examined below 1% concentration exhibits linearity as the palladium hydride exists purely in the alpha regime. Similarly, above 2% concentration, the hydride exists purely in the beta regime. The region between these regimes, the miscibility gap, is a coexisting mixture of both alpha and beta phases. Associated with the beta regime is an increase in the lattice parameter, affecting a more pronounced change in the optical properties.

Focusing on the low hydrogen concentration, beta region, we present in Fig. 8 the sensitivity response of our best performing nanotube sample. A linear trend-line displays a good fit, confirming we are operating in the alpha regime. The response of a 20nm sputtered thin film of palladium has been added for comparison, with a second linear trend-line. The interception of the trend-lines with the axis offers a suggestion as to the performance at very low concentrations. At the current state of development, the technology offers a three-fold increase in the sensitivity in this regime.

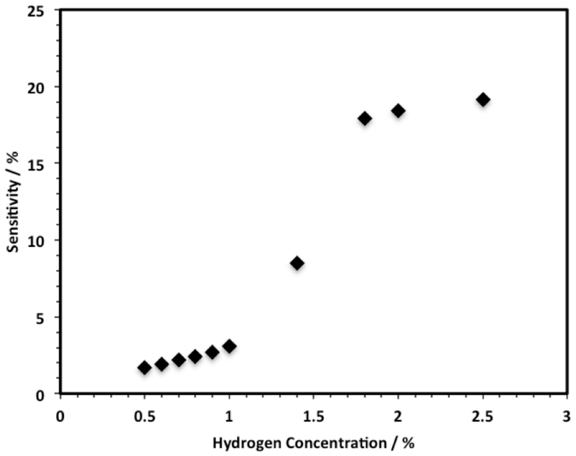

Figure 7. Sensitivity of palladium nanotubes extracted from Fig. 6.

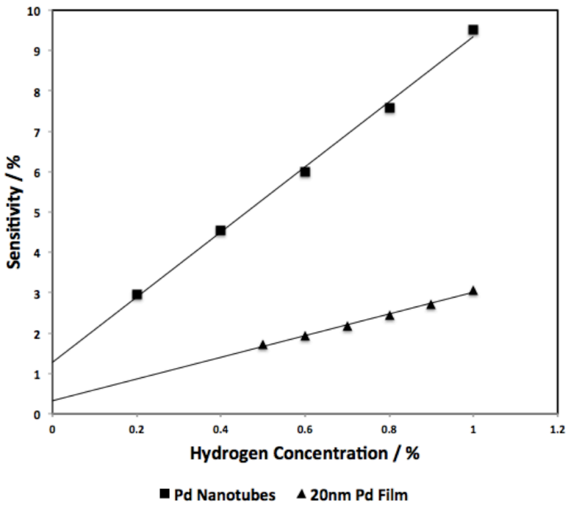

Figure 8. Sensitivity of nanotubes, compared to a sputtered 20nm palladium film, at concentrations less than 1% hydrogen in nitrogen.

V. FUTURE WORK

The next stage of this study will be to further characterise the nanostructures in a variety of ways. We plan to use finite element modeling and the available parameters in the fabrication process to investigate the optimal structural dimensions for sensitivity and reaction time. Through further optimisation of the fabrication process, we hope to improve the consistency of performance across all samples.

All experiments to this stage have been performed in a nitrogen carrier gas at ambient temperatures, however in real applications the sensor environment often contains known palladium contaminants such as hydrocarbons or sulphurs at elevated temperatures [14]. There is therefore a necessity to develop ways to enhance the selectivity and lifetime of structures exposed to poisoning gases.

VI. CONCLUSIONS

Freestanding upright palladium nanotubes have been fabricated and a range of post-fabrication techniques used to examine the absorption kinetics of the structure. The results suggest that nanotubes are advantageous to hydrogen sensing through massively increased absorption sites at both the inner and outer surface areas of the nanotube.

The nanotubes were characterised using stepped exposure profiles of hydrogen to find the alpha and beta regimes. In comparison with a 20nm palladium film, the best performing nanotube sample displayed sensitivities with a three-fold increase over the film.

REFERENCES

[1] M. a. Butler, "Optical fiber hydrogen sensor," *Appl. Phys. Lett.*, vol. 45, no. 10, p. 1007, 1984.

[2] K. Wyrzykowski, A. Rodzik, and B. Baranowski, "Optical transmission and reflection of PdHx thin films," *J. Phys. Condens. Matter*, vol. 2269, 1989.

[3] F. A. Lewis, *The Palladium Hydrogen System*, 1st ed. Academic Press Inc, 1967.

[4] T. Hübert, L. Boon-Brett, G. Black, and U. Banach, "Hydrogen sensors – A review," *Sensors Actuators B Chem.*, vol. 157, no. 2, pp. 329–352, Oct. 2011.

[5] S. Nazarpour, a. Cirera, and M. Varela, "Material properties of Au–Pd thin alloy films," *Thin Solid Films*, vol. 518, no. 20, pp. 5715–5719, Aug. 2010.

[6] X. Q. Zeng, M. L. Latimer, Z. L. Xiao, S. Panuganti, U. Welp, W. K. Kwok, and T. Xu, "Hydrogen gas sensing with networks of ultrasmall palladium nanowires formed on filtration membranes.," *Nano Lett.*, vol. 11, no. 1, pp. 262–8, Jan. 2011.

[7] A. Pundt, "Hydrogen in Nano-sized Metals," *Adv. Eng. Mater.*, vol. 6, no. 12, pp. 11–21, Feb. 2004.

[8] J. R. Pitts, P. Liu, S. Lee, C. E. Tracy, and A. Hopkins, "Interfacial Stability of Thin Film Hydrogen Sensors," *Proc. 2000 DOE Hydrog. Progr. Rev.*, pp. 1–16, 2000.

[9] P. Offermans, H. D. Tong, C. J. M. van Rijn, P. Merken, S. H. Brongersma, and M. Crego-Calama, "Ultralow-power hydrogen sensing with single palladium nanowires," *Appl. Phys. Lett.*, vol. 94, no. 22, p. 223110, 2009.

[10] N. Khosro Pour, F. Krummenacher, and M. Kayal, "An ultra-low power energy-efficient microsystem for hydrogen gas sensing applications," *Analog Integr. Circuits Signal Process.*, vol. 77, no. 2, pp. 155–168, Sep. 2013.

[11] A. Tittl, P. Mai, R. Taubert, D. Dregely, N. Liu, and H. Giessen, "Palladium-based plasmonic perfect absorber in the visible wavelength range and its application to hydrogen sensing.," *Nano Lett.*, vol. 11, no. 10, pp. 4366–9, Oct. 2011.

[12] S. H. Lim, B. Radha, J. Y. Chan, M. S. M. Saifullah, G. U. Kulkarni, and G. W. Ho, "Flexible palladium-based h2 sensor with fast response and low leakage detection by nanoimprint lithography.," *ACS Appl. Mater. Interfaces*, vol. 5, no. 15, pp. 7274–81, Aug. 2013.

[13] W. R. Hendren, A. Murphy, P. Evans, D. O. Connor, G. A. Wurtz, A. V Zayats, R. Atkinson, and R. J. Pollard, "Fabrication and optical properties of gold nanotube arrays," *J. Phys. Condens. Matter*, vol. 20, 2008.

[14] P. Albers, J. Pietsch, and S. F. Parker, "Poisoning and deactivation of palladium catalysts," *J. Mol. Catal. A Chem.*, vol. 173, no. 1–2, pp. 275–286, Sep. 2001.